Base excision repair of reactive oxygen species–initiated 7,8-dihydro-8-oxo-2′-deoxyguanosine inhibits the cytotoxicity of platinum anticancer drugs

Thomas J. Preston,[1] Jeffrey T. Henderson,[1] Gordon P. McCallum,[1] and Peter G. Wells[1,2]

[1]Faculty of Pharmacy and [2]Department of Pharmacology and Toxicology, University of Toronto, Toronto, Ontario, Canada

Abstract

Anticancer therapy with cisplatin and oxaliplatin is limited by toxicity and onset of tumor resistance. Both drugs form platinum-DNA cross-linked adducts, and cisplatin causes oxidative DNA damage including the 7,8-dihydro-8-oxo-2′-deoxyguanosine (8-oxodG) lesion. To assess oxidative DNA damage as a mechanism of cisplatin and oxaliplatin cytotoxicity, 8-oxodG–directed base excision repair was stably enhanced in human embryonic kidney cells by FLAG-tagged expression of human oxoguanine glycosylase 1 (α-OGG1) or its functional homologue, *Escherichia coli* formamidopyrimidine glycosylase (fpg). Both drugs increased reactive oxygen species and 8-oxodG levels, and cytotoxicity was decreased by antioxidant pretreatment. Ectopic expression of α-*OGG1* or *fpg* in cell clones increased nuclear and mitochondrial 8-oxodG repair, and reduced death by reactive oxygen species initiators (H_2O_2, menadione) and both platinum drugs. Exposure to oxaliplatin caused a more marked and sustained block of cell proliferation than exposure to cisplatin. We conclude that the 8-oxodG lesion is cytotoxic, and base excision repair a likely determinant of risk. The greater antitumor efficacy of oxaliplatin seems unrelated to oxidative DNA damage, suggesting a novel strategy for improving the therapeutic index in cancer therapy. [Mol Cancer Ther 2009;8 (7):2015–26]

Received 9/26/08; revised 4/6/09; accepted 4/7/09; published OnlineFirst 6/30/09.

Grant support: Canadian Institutes of Health Research, and the National Institute of Environmental Health Sciences (grant number 1-R21-ES013848-01A1). T.J. Preston and G.P. McCallum were supported by postdoctoral fellowships from the CIHR and the Rx&D Health Research Foundation.

The costs of publication of this article were defrayed in part by the payment of page charges. This article must therefore be hereby marked *advertisement* in accordance with 18 U.S.C. Section 1734 solely to indicate this fact.

Requests for reprints: Peter G. Wells, Faculty of Pharmacy, University of Toronto, 144 College Street, Toronto, ON, Canada M5S 3M2. Phone: 416-978-3221; Fax: 416-267-7797. E-mail: pg.wells@utoronto.ca

doi:10.1158/1535-7163.MCT-08-0929

Introduction

Oxidative stress can induce cell death through several mechanisms, including oxidative DNA damage. Reactive oxygen species (ROS)–induced nuclear and mitochondrial DNA damage is associated with the aging process as well as numerous pathologies in humans (1). The most common DNA base modification formed by oxidation is 7,8-dihydro-8-oxo-2′-deoxyguanosine (8-oxodG); thousands of these lesions may be formed in each cell daily and levels are increased upon exposure to a variety of xenobiotics (2). If unrepaired, postreplicative mispairing of 8-oxodG with adenine results in G:C to A:T transversion mutation (3). A major mechanism of directed prereplicative excision of 8-oxodG is the OGG1 glycosylase/apurinic/apyrimidinic (AP) lyase–initiated base excision repair (BER) pathway (4, 5). The importance of this specific enzymatic activity in 8-oxodG repair *in vitro* and *in vivo* has been well-characterized (6, 7). Overexpression of OGG1 (8, 9) or its functional bacterial homologue Fpg (10, 11) can protect against oxidative stress–induced 8-oxodG accumulation in cell culture and mouse models (12–14), and $ogg1^{-/-}$ knockout mice accumulate accelerated levels of 8-oxodG with aging and particularly after exposure to ROS-inducing drugs (15, 16). However, OGG1 overexpression has also been shown to promote cytotoxicity (17). In humans, defective 8-oxodG repair may increase susceptibility to cancer, as increased ROS-associated DNA alteration and mutation is thought to promote tumor initiation and progression. The *OGG1* locus maps to chromosome 3p26.2, a region frequently deleted in several tumor types (18). Additionally, epidemiologic studies support a correlation between the Ser326Cys polymorphism of OGG1, which down-regulates repair activity, and increased risk of carcinogenesis (19, 20). In clinical cancer treatment, a paradoxical association is proposed, with efficient BER of oxidative DNA damage promoting tumor resistance to specific anticancer therapies.

Cisplatin has been used extensively in the treatment of several cancer types. Although initial courses of cisplatin chemotherapy are usually effective, adverse side effects can limit drug use, and if disease progression occurs, tumor resistance to treatment is a common outcome (21). Reaction of cisplatin with purines to form DNA monoadducts that can mediate intrastrand and interstrand cross-links is essential for its cytotoxic activity (22). Platinum-DNA adducts are recognized by both the nucleotide excision repair (NER) and mismatch repair (MMR) pathways; however, removal of these macromolecular lesions by NER is often inefficient, and attempted MMR can actually promote cell death via induction of mitotic crisis (21, 22). Recent evidence indicates

that in addition to the classic mechanism of DNA cross-link formation, platinum compounds also induce free radical production leading to oxidative DNA damage. The high reactivity of cisplatin with thiols including glutathione and metallothioneins is protective, but if thiol capacity is overwhelmed, the disruption of cellular redox balance by cisplatin may promote cytotoxicity via oxidative stress (23, 24). Also, intracellular hydrated cisplatin itself may be capable of redox cycling. A number of studies *in vitro* and in animal models have shown that cisplatin exposure increases intracellular levels of ROS in tissues, and that antioxidant therapy using a variety of free radical scavengers protects against cisplatin-mediated toxicities (25–28). Therefore in addition to NER and MMR, altered BER capacity may also modulate the response to cisplatin therapy; however, this has not been directly tested.

Current clinical use of the newer generation platinum analogue oxaliplatin in combination chemotherapy exhibits increased efficacy in the treatment of cisplatin-resistant cancers. In initial drug screening experiments, oxaliplatin displayed a spectrum of activity distinct from that in first- and second-generation platinum compounds, facilitating reduced cross-resistance in cisplatin-insensitive cancer cell lines (29). The molecular mechanisms underlying this improved potency remain to be fully identified. Although oxaliplatin produces less platinum-DNA adducts and interstrand DNA cross-links than equimolar concentrations of cisplatin, it is highly cytotoxic (23). Upon reaction with DNA, the bulky diaminocyclohexane moiety of oxaliplatin may induce a unique repair response that may account for the increased tumor sensitivities observed (30). For example, guanine diadducts formed after oxaliplatin-DNA reaction seem to be recognized exclusively by the NER pathway (31). Cancer cells exhibiting MMR response down-regulation that are resistant to cisplatin treatment would accordingly remain susceptible to oxaliplatin-mediated destruction. A recent clinical study indicates that, as observed with cisplatin, oxidative stress may constitute a mechanism of neurotoxicity associated with oxaliplatin therapy (32).

In the present study, we examined the specific role of the 8-oxodG lesion in platinum compound toxicity, distinct from other protein or DNA adduct formation. The ability of stably-induced BER of 8-oxodG to alter cytotoxicity from acute exposure to ROS (H_2O_2) or a redox-cycling quinone (menadione; ref. 33), and to cisplatin or oxaliplatin, was evaluated in a human cell culture (HEK 293) model. Enhancement of BER activity was accomplished via stable ectopic expression of bacterial (*fpg-FLAG-NLS*) or human (*α-OGG1-FLAG*) glycosylase/AP lyase constructs in a series of cell clones. Increased 8-oxodG excision activity by Fpg and α-OGG1 was observed in both the nuclear and mitochondrial compartments, and these activities reduced both endogenous and drug-induced 8-oxodG levels. The majority of *fpg-FLAG-NLS* and *α-OGG1-FLAG* clones displayed significantly increased resistance to all treatments. Protection against cisplatin-mediated cytotoxicity was more robust than that observed with oxaliplatin treatment. Pretreatment with the H_2O_2 scavenger catalase also reduced cell death from exposure to both platinum compounds. Intracellular ROS and nuclear 8-oxodG levels were increased by cisplatin and to a slightly lesser extent by oxaliplatin. 8-OxodG level induction associated with cytotoxicity was immediate and subsided within the first hour after acute treatments, unlike a more prolonged increase in ROS production. The results identify 8-oxodG production as a mechanism of the cytotoxic activity of platinum drugs and BER capacity as a determinant of cellular response to platinum drug exposure. A larger role for the 8-oxodG lesion in the cytotoxicity of cisplatin compared with the more efficacious oxaliplatin suggests that treatments less reliant upon oxidative DNA damage for the induction of target cell death may improve anticancer therapy.

Materials and Methods

Cell Culture and Reagents

Human embryonic kidney cells (HEK 293; ATCC CRL-1573) and derived clones were propagated in minimal essential media (Eagle α modification) plus 2 mmol/L L-glutamine, 1% penicillin/streptomycin solution (Sigma-Aldrich), and 10% heat-inactivated fetal bovine serum (Hyclone). Cultures were maintained in a humidified incubator at 37°C with 95% air, 5% CO_2 (B.O.C./Canox). Thirty percent H_2O_2 solution, menadione, cisplatin and oxaliplatin were from Sigma-Aldrich.

Expression Vectors and Cell Transfections

The pC3/pCAGGS expression vector was constructed by ligation of PvuI and EcoRI digest fragments from pcDNA3 (Invitrogen) and pCAGGS (34). *Escherichia coli fpg* cDNA was obtained as described (14) and human *α-OGG1* cDNA was produced from HEK 293 cell mRNA using MBI Fermentas first strand cDNA synthesis kit and sequence-specific PCR. FLAG tag sequence (Sigma-Aldrich), SV40 Large Tumor Antigen nuclear localization signal (SV40 LT NLS) sequence, and EcoRI sites were added to cDNAs by sequence-specific PCR. cDNAs were incorporated into the EcoRI site of the pC3/pCAGGS multiple cloning site. Competent DH5α bacteria (Invitrogen) were transformed for plasmid propagation. Sequencing was done at the Centre for Applied Genomics, Hospital for Sick Children, Toronto. HEK 293 cells were transfected with plasmids using TransFectin lipid reagent protocol (Bio-Rad), and stable clones selected with 800 to 1,000 μg/mL G418 disulfate (Sigma-Aldrich).

Immunocytochemistry and Immunoblotting

Antibodies for FLAG tag (M2 mouse monoclonal; Sigma-Aldrich), *E. coli* Fpg (rabbit polyclonal; R+D Systems), human α-OGG1 (pAb rabbit polyclonal; Novus Biologicals), human proliferating cell nuclear antigen (mouse monoclonal 610664; BD Biosciences), and activated caspase-3 (rabbit polyclonal #9661; Cell Signaling Technology, Inc.) were used. For immunocytochemical analysis, cells were fixed in 4% paraformaldehyde, and endogenous peroxidase activity quenched with 0.1% H_2O_2. Cells were incubated in avidin D/MOM IgG blocking reagent (Vector

Laboratories), followed by primary antibody incubation (anti-FLAG Ab). Biotinylated (horse) anti-mouse secondary antibody, Vectastain Elite ABC reagents, and diaminobenzamide tetrachloride horseradish peroxidase substrate kit were from Vector Laboratories, Inc. Staining protocol was as directed. For Western blotting, preparation of nuclear and mitochondrial fractions were done as described (35). Fifty micrograms of each protein lysate sample were loaded per well of a 10% polyacrylamide gel for SDS-PAGE (Bio-Rad Mini Trans-Blot system) and transferred onto a nitrocellulose membrane (Bio-Rad). After antigen blocking and antibody incubations, enhanced chemiluminescence (ECL detection reagents; Amersham Biosciences) and exposure onto Bioflex MSI film (Clonex) were used for detection.

8-OxodG Incision Activity Assay

Protein lysates were prepared as described under *Immunochemistry and immunoblotting*. Lysis buffer was a negative control for 8-oxodG incision, and 5 units of Fpg enzyme (R+D Systems), a positive control. Buffers and polyacrylamide gels were as described (9). 49mer oligonucleotide containing 8-oxodG at base 22 was synthesized by Sigma Genosys; 10 pmol of this oligonucleotide was labeled with 50 μCi γ-^{32}P-ATP (Amersham Pharmacia) in a 10 μL, 30-min T4 polynucleotide kinase (Invitrogen) reaction, followed by heat-inactivation. Twenty microliters of annealing buffer were added and sample run through Bio-Rad Micro-Spin 6 columns for removal of free ATP. Complementary oligonucleotide (100 pmol; Sigma Genosys) was added, and samples were heated at 95°C for 5 min and then cooled. Three-hour repair reactions (20 μL) at 37°C each contained 1 μL of annealed oligonucleotide and 20 μg sample lysate in repair enzyme buffer (Trevigen). Reactions were stopped with 10 μL 3× gel loading buffer and heating at 95°C for 5 min. Samples were placed on ice, loaded onto prerun (150 V, 1 h, in Tris-borate EDTA buffer) 20% polyacrylamide gels, and resolved by eletrophoresis (150 V for 1.5 h). Gels were dried (Bio-Rad gel dryer) and labeled oligonucleotides observed by autoradiogram (Bioflex MSI film; Clonex). Densitometry of scanned autoradiogram films was done using NIH Image J 1.34s software.

Cell Viability and Toxicity Assays

Colony-forming assay was done as follows: 100 cells per well, six-well tissue culture plates (Becton Dickinson) were allowed to adhere overnight. Cells were exposed to drug for 1 h and cultures then incubated for 6 d. Wells were washed with PBS and cells fixed and stained in 0.5% methylene blue, 100% methanol for 15 min. Dye was removed with washes in double-distilled water and cell colonies were counted. For the colony-forming assay, the size of clonal colonies after 6 d of growth was optimal for counting of individual viable colonies. For the viability assay, the density of control (untreated) cells in each well was approaching 100% confluence after 6 d of growth. The Hoechst bisbenzimide 33258 (Sigma-Aldrich) fluorimetric assay for cell viability was done as described (36). Fifteen thousand cells per well (96-well plate; Becton Dickinson) were allowed to adhere and treated for 1 h (± 6-h preincubation with PEG-Catalase; Sigma-Aldrich). Sixteen hours after treatment, fluorescence was measured using a SpectraMAX Gemini XS microplate spectrofluorometer (Molecular Devices), and data were analyzed with SOFTmax Pro 3.1.2 analysis software (Molecular Devices). Lactate dehydrogenase (LDH) release was measured using CytoTox-ONE homogeneous membrane integrity assay (Promega). Ten thousand cells per well (96-well plate) were allowed to adhere and treated. Nine percent w/v Triton X-100 was a positive control for cell membrane rupture. At selected times after treatment, resazurin substrate was added and LDH-catalyzed fluorescence was measured.

ROS, 8-oxodG, and AP-Site Measurement

For measurement of intracellular ROS, 20,000 cells per well (96-well plate) were allowed to adhere and treated for 1 h. One hour after treatment, media was removed and replaced with PBS, and 5- (and-6) chloromethyl-2′,7′-dichlorodihydrofluorescein (Molecular Probes) added to a final concentration of 25 μg/mL. ROS-dependent conversion of DCF-DA to fluorescent product was quantified immediately and hourly (excitation, 485 nm; emission, 530 nm). For 8-oxodG level analysis, 2×10^5 cells were treated as indicated and nucleic acids extracted in 1.5 mL tubes by sodium iodide extraction protocol (37). Cell pellets were homogenized in lysis buffer, centrifuged at 800 × *g*, and resuspended in enzyme reaction solution. Samples were rehomogenized, incubated with RNase A and T, (Roche) and then with proteinase K (Roche; 1 h, 50°C each). Excess sodium iodide solution was added, DNA was precipitated and resuspended in Na-acetate buffer, and samples were briefly sonicated. Normalization for total DNA concentration between samples was determined by UV spectrophotometry. Nuclease P1 was added (2 h, 37°C) followed by alkaline phosphatase (Roche; 1 h, 37°C), and samples filtered through Millipore Microcon YM-10 columns (14,000 × *g*, 1 h). Fifty micrograms of each nucleotide sample were analyzed for 8-oxodG content (ng/mL) using a "highly sensitive" 8-OHdG check ELISA kit (Genox Corp.). Samples were ethanol cleaned and dG concentration measured by high performance liquid chromatography [tandem 5 μm ODS-2 spherisorb columns (Waters); Perkin-Elmer series 200 UV detector] to normalize for nucleotide digestion. For AP-site analysis, 2×10^5 cells were treated as indicated and nucleic acids were extracted with a GenElute Mammalian Genomic DNA Miniprep kit (Sigma Genosys). AP sites were quantified via the Aldehyde Reactive Probe method using a commercially available kit (Biovision, Inc.).

Statistical Analysis

Data graphing and statistical analysis were done using GraphPad PRISM 3.02 and GraphPad InStat 3.0 software. Means and SDs for all measured biological parameters are displayed in the appropriate graphs. Significant differences in a single parameter (i.e., treated versus untreated) between samples were determined by one-way ANOVA and Tukey's multiple comparison test. Significant differences in two parameters (i.e., treatment and time) between samples

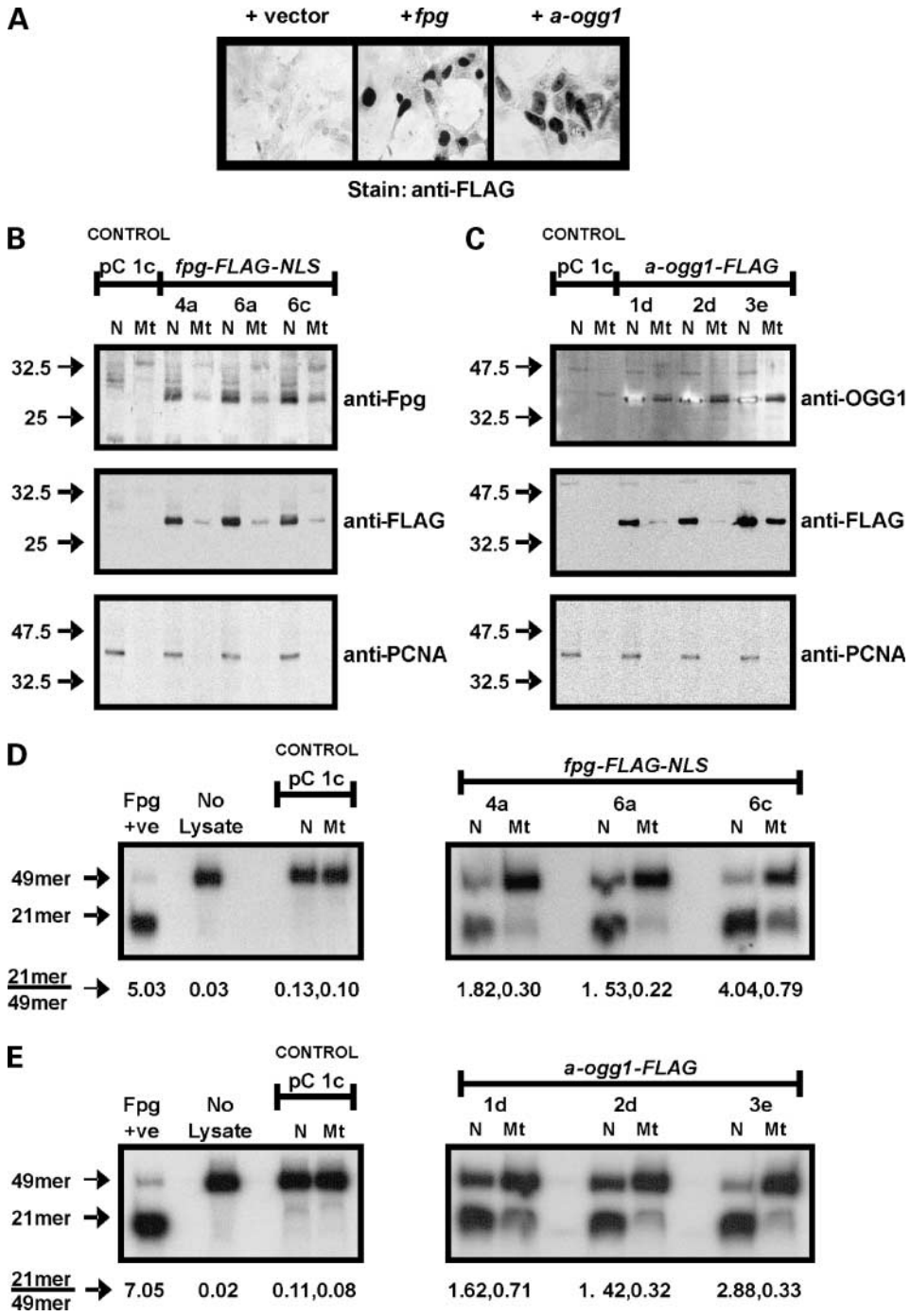

Figure 1. Expression, subcellular localization, and activity of Fpg-FLAG-NLS and α-OGG1-FLAG in stable HEK 293 clones. **A,** detection of FLAG-tagged ectopic protein expression by immunocytochemistry (transient transfections). **B** and **C,** stable expression of Fpg-FLAG-NLS (**B**) and α-OGG1-FLAG (**C**) in both nuclear (*N*) and mitochondrial (*Mt*) compartments, as observed with detection of ectopic proteins and FLAG tag by Western blotting. Membranes were reprobed for proliferating cell nuclear antigen (*PCNA*) to confirm purity of subcellular fractions. **D** and **E,** *in vitro* 8-oxodG incision assay shows increased 8-oxodG repair activity in nuclear and mitochondrial lysates from *fpg* (**D**) and *α-OGG1* (**E**) clones. Values beneath sample lanes represent the ratio of cut (*21mer*) to uncut (*49mer*) substrate as determined by densitometry.

were determined by two-way ANOVA and Bonferroni post tests. To determine significant differences in treatment concentrations required to reduce cell survival by 50% (LC_{50}) between groups, log transformation of drug dose was done, and colony-forming counts were normalized to percent survival (0–100% parameters). The resulting curves were analyzed by nonlinear regression and multiple groups compared by one-way ANOVA.

Results and Discussion

Characterization of Transgenic Cell Clones Possessing Enhanced BER of the 8-oxodG Lesion

The experimental model in this study uses two distinct 8-oxodG glycosylase/AP lyase functional homologues, *E. coli* Fpg and human α-OGG1, for up-regulation of BER. Overexpression of Fpg and OGG1 protects against cytotoxicity resulting from xenobiotic-induced oxidative stress (12–14). We generated six independent stably transfected cell clones, three each for expression of FLAG-tagged *E. coli* Fpg (clones *fpg* 4a, 6a, 6c) or FLAG-tagged human α-OGG1 (clones 1d, 2d, 3e). The α isoform (transcript variant 1a) of OGG1 was

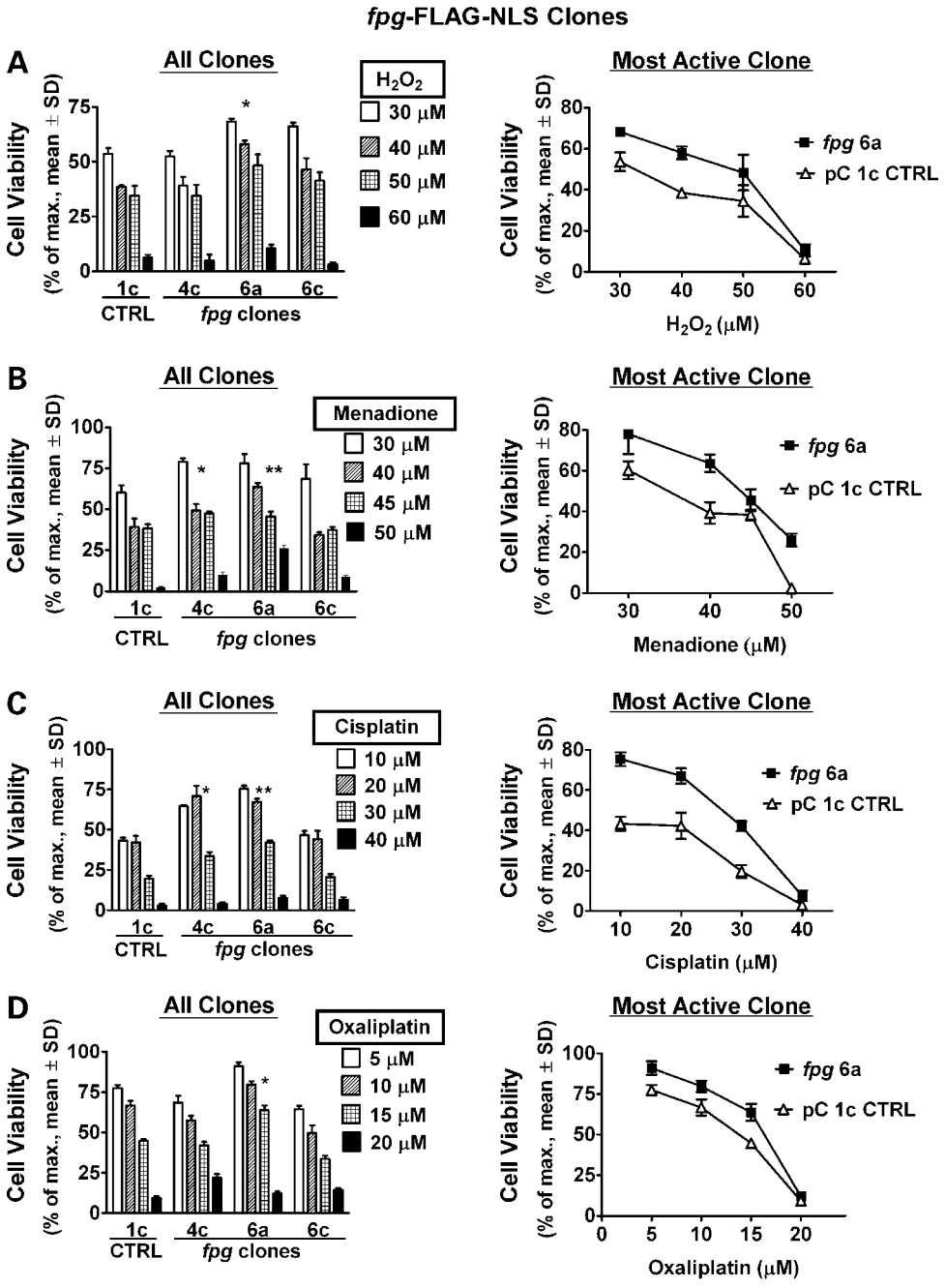

Figure 2. Increased 8-oxodG repair via ectopic Fpg expression inhibits cytotoxicity from acute exposure to ROS and ROS-inducing drugs. **A** to **D,** cell viability of stable *fpg*-expressing clones was compared with pC 1c control cells by colony forming assays, 7 d after 1 h exposure to the indicated concentrations of H_2O_2 (**A**), menadione (**B**), cisplatin (**C**), and oxaliplatin (**D**). Viability response for all clones (*left*) and survival curve of control versus most active clone (*right*) is shown. Specific clones with enhanced glycosylase/AP lyase activity exhibit increased resistance to most or all treatments. * and **, $P < 0.05$ of LC_{50} comparable with control.

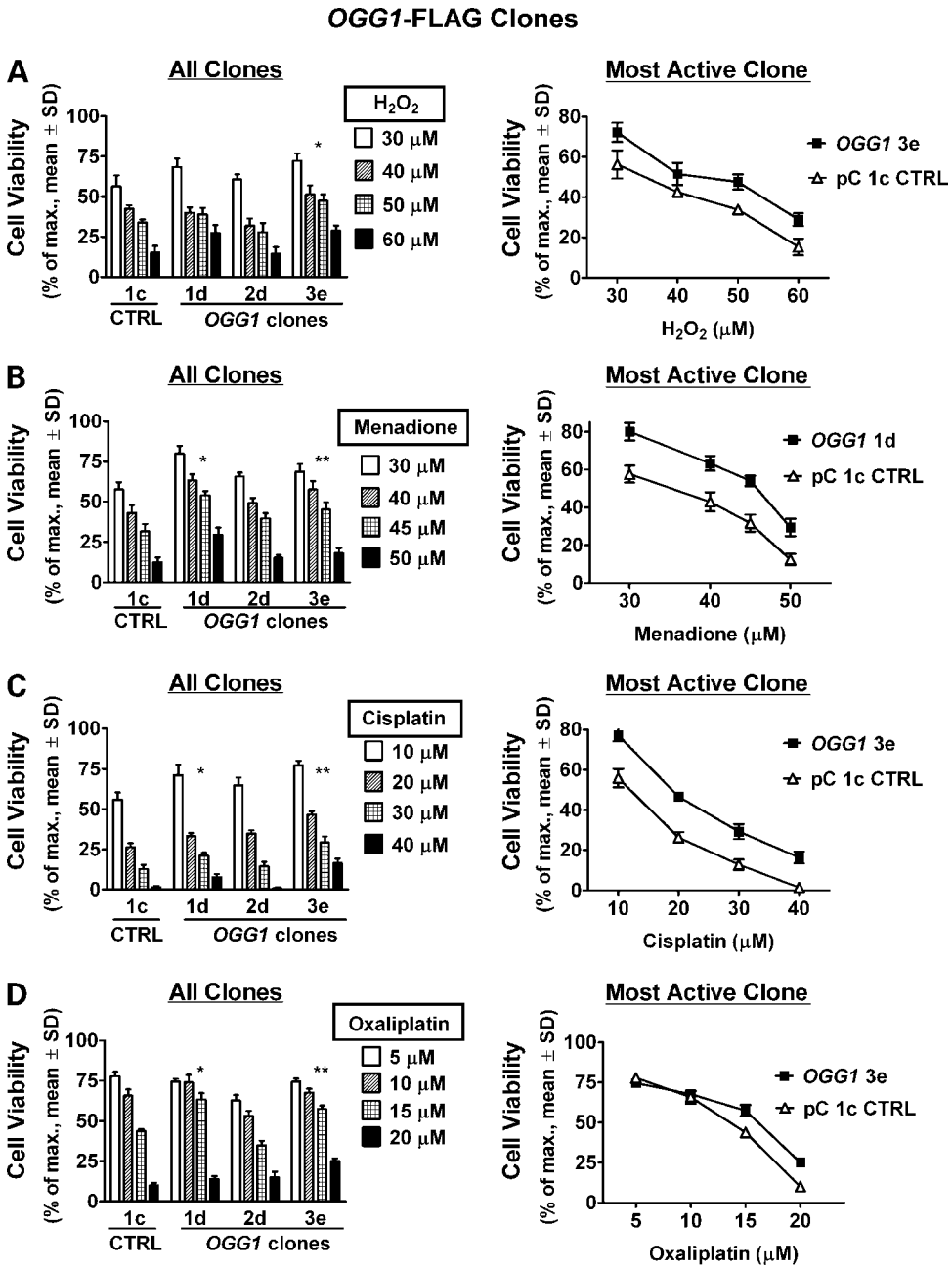

Figure 3. Increased 8-oxodG repair via ectopic α-OGG1 expression inhibits cytotoxicity from acute exposure to ROS and ROS-inducing drugs. **A** to **D,** cell viability of stable *α-OGG1*–expressing clones was compared with pC 1c control cells by colony forming assays, 7 d after 1 h exposure to the indicated concentrations of H_2O_2 (**A**), menadione (**B**), cisplatin (**C**), and oxaliplatin (**D**). Viability response for all clones (*left*) and survival curve of control versus most active clone (*right*) are shown. Specific clones with enhanced glycosylase/AP lyase activity exhibit increased resistance to most or all treatments. * and **, $P < 0.05$ of LC_{50} comparable with control.

used as it displays DNA glycosylase activity in both the nucleus and mitochondria, as opposed to the mitochondria-localized β-OGG1 (transcript variant 2a), which has been reported to lack such activity (38). Detection of ectopic Fpg and α-OGG1 by immunocytochemistry and immunoblotting was aided by incorporation of a FLAG tag sequence into the 3′ end of transgene cDNA, for detection of protein products by a monoclonal anti-FLAG antibody. FLAG epitope addition did not inhibit the enzymatic activity of transgene products. Robust expression and nuclear localization of transgene products were observed (Fig. 1A). High level nuclear and lower level mitochondrial localization of transgene expression was confirmed in *fpg* clones (Fig. 1B) and *OGG1* clones (Fig. 1C) by immunoblotting of fractionated

cell protein lysates for both enzyme and FLAG epitopes. Reprobing for nuclear proliferating cell nuclear antigen indicated the purity of sample lysate fractions. The presence of Fpg in the mitochondrial fraction was unexpected, as unlike OGG1, Fpg does not possess a mitochondrial targeting signal. However, a mitochondrial targeting signal is not essential for proteins to localize to mitochondria and be identified in the mitochondrial compartment as assessed by immunoblotting/immunochemical staining (39–41). It was not determined if Fpg was present in the mitochondrial matrix.

All *fpg* and *OGG1* clones displayed markedly increased 8-oxodG:C-directed glycosylase/AP lyase activity in the nucleus and mitochondria compared with the pC 1c control (Fig. 1D and E). Activity was induced approximately 10- to 30-fold (nucleus) and 2- to 8-fold (mitochondria) by Fpg-FLAG-NLS, and approximately 12- to 25-fold (nucleus) and 2- to 7-fold (mitochondria) by α-OGG1-FLAG. Thus, stable ectopic expression of either functional homologue up-regulated BER-directed repair of 8-oxodG to a comparable degree in our model system. Increased glycosylase/AP lyase activities in *fpg* and *OGG1* cell clones induced 8-oxodG repair; however, overexpression of one component of the BER pathway in the absence of adequate levels of other enzymes in the pathway may cause deleterious effects through the accumulation of toxic repair intermediates. For example, overexpression of MAG 3-methyladenine DNA glycosylase in AP endonuclease activity–deficient yeast cells increases spontaneous mutation frequency, presumably due to an inability to repair glycosylase-generated abasic sites in the absence of endonuclease activity (42). Overexpression of OGG1 in HEK 293 clones did not increase total AP site levels, and these levels were only slightly elevated with overexpression of Fpg (Supplementary Fig. S1).[3] This is consistent with studies in human B-lymphoblastoid TK6 cells where no increase in double strand breaks are observed in untreated hOGG1 overexpressing cells compared with control cells (43, 44). In addition, stable expression of *Fpg* and *OGG1* transgenes did not affect HEK 293 clone morphology, adherence, proliferative capacity, or viability, consistent with observations in other cells (12–14, 45). Overexpression of hOGG1 in human B-lymphoblastoid TK6 cells protects the cells from exposure to H_2O_2, which predominantly generates single site DNA lesions; however, this sensitizes the cells to γ-radiation, possibly through the formation of radiation-specific cluster lesions that may be converted into lethal double strand breaks by abortive BER (43, 44, 46). Holt and Georgakalis (47) have shown that human acute lymphoblastic leukemia pre–B NALM6 cell treatment with γ radiation but not H_2O_2 results in the induction of oxypurine cluster lesions. Intriguingly, exposure of radiation-resistant human 28SC monocytes to therapeutic doses of γ-radiation increases levels of persistent abasic cluster lesions without any resulting production of double strand breaks, indicating that cluster lesions themselves may mediate cytotoxicity (48).

Fpg and αOGG1 Activities Inhibit Cell Death from Acute ROS and ROS-Inducing Drug Exposures

As ROS and ROS-initiating drugs induce the 8-oxodG lesion, the response of cell clones stably expressing Fpg and αOGG1 to exposure to ROS (H_2O_2), a redox cycling and adduct forming quinone (menadione; ref. 33), and adduct forming cisplatin (23, 24) was investigated and compared with the response to oxaliplatin. In addition to the well-documented DNA cross-link formation by cisplatin-DNA monoadduct reactions, the induction of free radicals leading to oxidative DNA damage and the inhibition of oxidative DNA damage repair may also contribute to its cytotoxic activity (21, 49). Oxaliplatin also forms adducts with DNA and is reported to stimulate intracellular ROS production (50). Survival of HEK 293 clones exposed to a concentration range of acute (1 hour) treatments was assessed by colony-forming assay (Figs. 2 and 3). Cytotoxicity of all treatments was reduced in the majority of both *fpg* (Fig. 2, clones 4c and 6a) and *OGG1* (Fig. 3, clones 1d and 3e) clones compared with the pC 1c empty vector control. At high dose levels, the viability of *fpg* clones was lower than *OGG1* clones. This may be a result of differential substrate specificity of the two enzymes, or the low AP lyase activity of OGG1 in the absence of comparable levels of AP endonuclease 1 (51). With increasing 8-oxodG levels at high doses, efficient AP lyase activity (Fpg) in the absence of appropriate downstream repair may result in the promotion of lethal DNA damage (44, 51). The functional redundancy obtained using two models of 8-oxodG glycosylase/AP lyase up-regulation (Fpg and α-OGG1) shows a common mechanism of 8-oxodG–directed, BER-mediated resistance to this variety of oxidative stressors. Like platinum drugs, menadione is a source of intracellular ROS and can affect cellular redox balance by adduct formation with proteins and DNA. The coresistance of cell clones exhibiting enhanced BER to platinum drugs and menadione that we observe is in support of such a common mechanism of action. All cell clones were more sensitive to oxaliplatin treatment than to cisplatin treatment. Twice the concentration range (10–40 μmol/L) of cisplatin was required to induce levels of cell death comparable with oxaliplatin (5–20 μmol/L). As well, treatment-resistant *fpg* and *OGG1* clones exhibited an approximate 2-fold increase in colony survival after cisplatin exposure (Figs. 2C and 3C), whereas this survival increase was marginal following oxaliplatin exposure (Figs. 2D and 3D). These disparities indicate differences in the mechanisms of cytotoxicity for these two platinum compounds that are independent of BER capacity.

Differential Response of Cell Clones to Cytotoxic and Cytostatic Effects of Cisplatin or Oxaliplatin Treatment

Our study reveals a differential cellular response to cisplatin versus oxaliplatin; specifically, increased sensitivity to both the cytotoxic and cytostatic activities of oxaliplatin seems to be independent of oxidative stress and 8-oxodG. One *fpg* and one *OGG1* clone exhibiting comparable resistance to platinum compounds were used for further analysis

[3] Supplementary material for this article is available at Molecular Cancer Therapeutics Online (http://mct.aacrjournals.org/).

of drug effects. To determine the temporal onset of drug-induced cell death, viable cell numbers were quantified 16 hours after treatment and compared with untreated control (Fig. 4A and B). The reduction in viable cells observed at this time point compared with that observed by colony forming assay. This indicates that cytotoxicity was rapid and independent of 8-oxodG–mediated G:C to A:T transversion mutations, as the average period of HEK cell division was ~24 hours. A high (2-fold) increase in resistance to cisplatin (Fig. 4A) and lower (1.2-fold) increase in resistance to oxaliplatin (Fig. 4B) in *fpg* 6a and *OGG1* 1d clones was reconfirmed. LDH release from the cytosol into the culture media was measured as a marker of cytotoxicity at selected time points during the initial 24 hours following drug administration (Fig. 4C). LDH release was modestly enhanced at 4 hours by both drugs, with a maximal increase from cisplatin exposure observed after 12 hours (~120% over untreated), and a maximal increase from oxaliplatin exposure after 24 hours (~ 50% over untreated). The relatively low enhancement of LDH release overall compared with untreated samples was consistent with a lack of necrotic cell morphology observed in cultures. Immunohistochemical staining for activated caspase-3 in PC 1c control cells revealed a 3.8- and 5.6-fold increase in the percentage of positive cells 16 hours following treatment with cisplatin and oxaliplatin, respectively (Supplementary Fig. S2).[3] These observations are

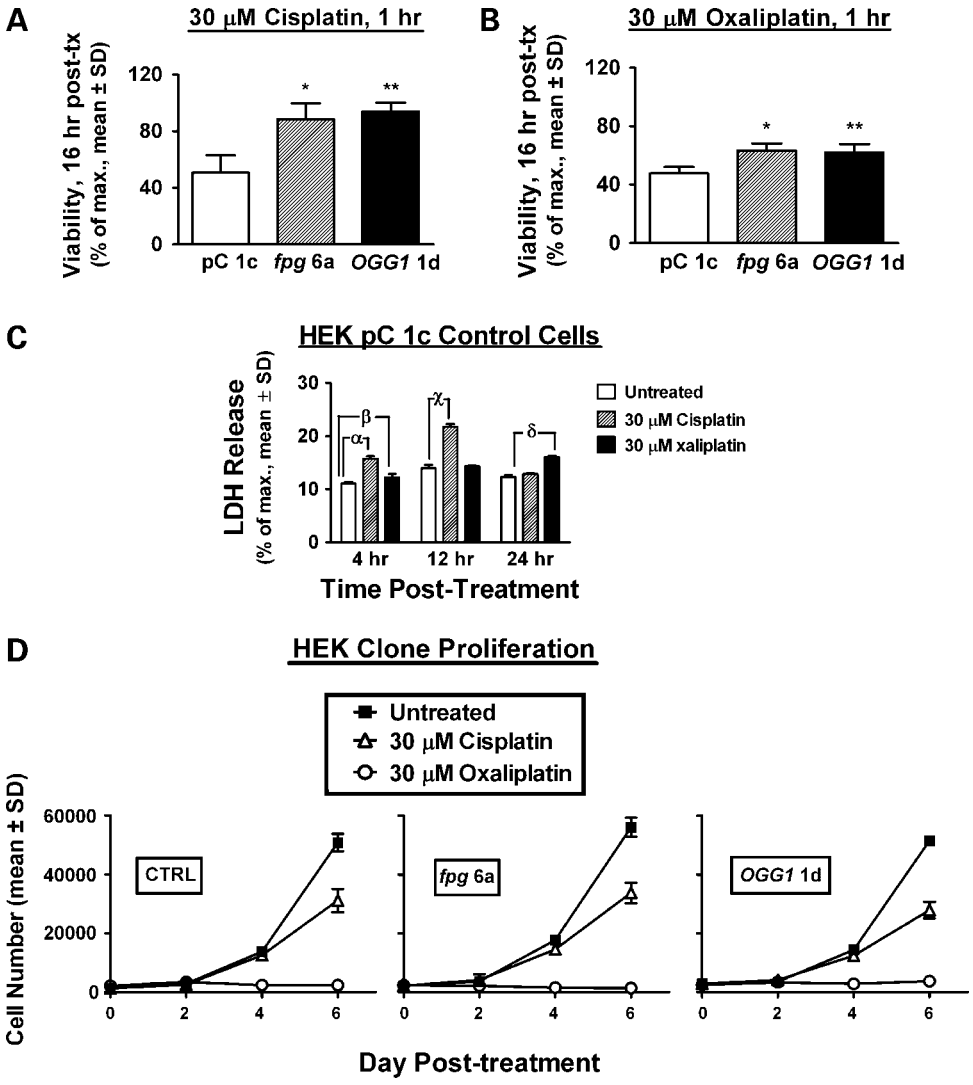

Figure 4. 8-OxodG–mediated cell death occurs within 24 h of acute exposure to cisplatin and oxaliplatin and is distinct from differential effects of each drug upon cell proliferation. **A** and **B,** viability of selected *fpg* and *α-OGG1* clones was compared with control 16 h after cisplatin (**A**) or oxaliplatin (**B**) treatment as measured by cell number (Hoechst fluorescence). **C,** cell membrane damage-mediated LDH release into the culture media after 1 h exposure of HEK pC 1c cells to the indicated dose of platinum compounds at 4, 12, and 24 h after treatment. LDH release was compared with untreated control. **D,** effects of cisplatin and oxaliplatin exposure (30 μmol/L, 1 h) upon selected HEK clone proliferation over 6 d after treatment (cell number determined by Hoechst fluorescence). * and **, $P < 0.05$ compared with control. α, β, χ, and δ, $P < 0.05$ compared with control.

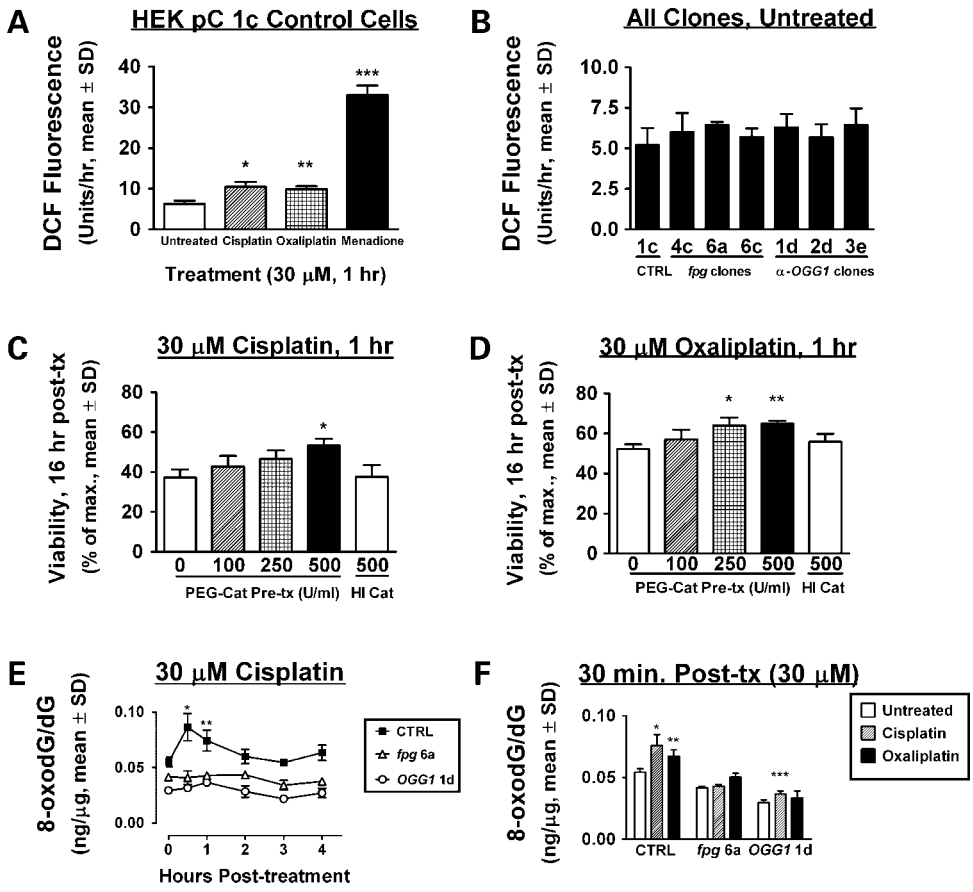

Figure 5. Platinum compounds increase intracellular ROS and nuclear 8-oxodG levels, and cytotoxicity is reduced with both enhanced BER and antioxidant therapy. **A** and **B,** ROS production in pC 1c control (**A**) and all (**B**) cell clones was measured by CM-H_2DCF-DA fluorescence 1 to 4 h after the indicated treatments. **C** and **D,** viability of HEK pC 1c cells 16 h after exposure to cisplatin (30 μmol/L, 1 h; **C**) or oxaliplatin (30 μmol/L, 1 h; **D**) assessed by cell number (Hoechst fluorescence). Cultures were pretreated for 6 h with the indicated dose of PEG-Catalase (*cat*) or heat-inactivated (*HI*) PEG-Cat. **E** and **F,** time course of nuclear 8-oxodG levels (ng 8-oxodG per μg dG) in untreated (displayed as "time 0") cell clones and 0.5 to 4 h after cisplatin treatment (30 μmol/L, 1 h; **E**). Nuclear 8-oxodG levels in untreated clones or 30 min after treatment with the indicated agents (all 30 μmol/L, 1 h; **F**). *, **, and ***, $P < 0.05$ compared with untreated.

consistent with a recent report showing p53-dependent apoptosis in cisplatin treated HEK 293 cells (52).

The rapid onset of cell death observed from acute platinum drug exposure suggests that cell death may have resulted from a stress response caused by cell cycle arrest. HEK clone proliferative capacity after drug treatment was observed by quantifying cell numbers over 6 days (Fig. 4D). After initial cell loss, cisplatin inhibited the proliferation of all clones tested (including control) by ~50%. In contrast, the cytostatic effect of oxaliplatin upon all clones was more potent, with an almost complete block of cell division over 6 days that resumed 7 to 8 days after treatment. These diverse activities of cisplatin and oxaliplatin on clonal proliferation seem to be independent of 8-oxodG–mediated effects, as all cells reacted in a similar fashion regardless of stable BER transgene expression. In clinical anticancer therapy, similar doses of cisplatin (75 mg/m^2) or oxaliplatin (60 mg/m^2) have been given without causing significant adverse toxicity (53, 54). Thus, the enhanced efficacy of oxaliplatin therapy in the treatment of cisplatin-resistant cancers may relate to a higher level of cytotoxicity in tumors at comparable drug concentration.

Antioxidant Therapy Protects Against Death by Platinum Drug-induced Intracellular ROS

To confirm that the altered responses of *fpg* and *OGG1* clones to platinum drug therapy resulted from BER-mediated resistance to ROS-induced 8-oxodG accumulation, the ability of cisplatin and oxaliplatin to increase intracellular ROS and 8-oxodG levels, and the effect of antioxidant pretreatment on cytotoxicity were assessed. pC 1c cells were exposed to 30 μmol/L cisplatin, oxaliplatin, or menadione for 1 hour, and the generation of ROS in cultures was quantified by intracellular DCF-DA fluorescence (Fig. 5A). ROS accumulation over 3 hours was increased 2-fold by both cisplatin and oxaliplatin treatments, and to a greater extent (~6-fold) by exposure to menadione. DCF-DA fluorescence from all clones (untreated) was analyzed to ensure that transgene introduction was not itself altering basal intracellular ROS levels (Fig. 5B). All clones produced comparable levels of ROS in culture. The contribution of ROS level

enhancement by platinum drugs to their cytotoxic activities was assessed. The effect of preincubation with a membrane-permeable conjugate of the H_2O_2 scavenging enzyme catalase (PEG-Cat) before exposure to platinum compounds on cell viability was measured (Fig. 5C and D). Increasing catalase concentration (100–500 U/mL of culture media) produced comparable increases in resistance (approximately 10–20%) to cisplatin and oxaliplatin, whereas 500 U/mL of heat-inactivated catalase had no such effect. These results indicate that ROS production is a cytotoxic mechanism for both platinum compounds in our model. This comparable degree of protection conferred by catalase reflects the comparable level of ROS induction by both drugs.

BER Up-Regulation Lowers Endogenous 8-oxodG Levels and Blocks Rapid 8-oxodG Accumulation from Platinum Drug Treatment

Cisplatin is reported to increase intracellular ROS and 8-oxodG levels (27). As Fpg and α-OGG1 overexpression has been shown to lower 8-oxodG and oxypurine-clustered DNA damage levels, and *OGG1*-deficient mice exhibit tissue-specific increases in 8-oxodG accumulation following ROS-inducing xenobiotic exposure (12–16, 55), we measured nuclear 8-oxodG/dG ratios in untreated and drug-treated cell clones (Fig. 5E and F). Ectopic expression of Fpg (clone *fpg* 6a) or α-OGG1 (clone *OGG*1 1d) significantly lowered endogenous nuclear 8-oxodG levels compared with the pC 1c clone control. In addition, stable transgene expression markedly inhibited an immediate increase in 8-oxodG generation following cisplatin treatment (30 μmol/L; Fig. 5E). A maximal 1.5-fold increase in 8-oxodG/dG occurred 30 minutes after treatment compared with untreated sample and was diminished by 2 hours after treatment. Oxaliplatin exposure produced a slightly lower increase in 8-oxodG/dG that also was inhibited in *fpg* and α-*OGG1* transgenic clones. The rapid and temporary increase in nuclear 8-oxodG levels observed following treatment with both platinum drugs indicates that this DNA lesion was not a result of intracellular oxidative stress via platinum adduct formation with cellular thiols such as glutathione.

Many anticancer therapies including cisplatin treatment destroy tumor cells at least in part through the induction of acute oxidative stress (21, 24). However, nontoxic oxidative stress is also associated with cancer initiation and progression, as ROS can induce carcinogenic DNA mutation and stimulate cell survival and proliferation (18, 36). Indeed, a variety of antioxidants are currently being tested for their prophylactic potential and as adjunct therapies in the treatment of existing cancers (56). This raises the potential dilemma of antioxidants blocking the anticancer effect of a drug that relies upon toxic ROS accumulation for cancer cell destruction. Our results indicate that antioxidant therapy may affect platinum drug activities. The specific promotion of the 8-oxodG lesion by ROS as a mechanism of drug toxicity has been well-characterized (57, 58). Here, we provide additional evidence for this mechanism in platinum drug toxicity. 8-OxodG induction is not indicated as the sole factor causing the premitotic onset of cytotoxicity in our experimental model. The reported modulation of cisplatin toxicity by cellular signal transduction cascades independent of a DNA damage response implicates other stress pathways as part of this process. One such signal is the c-Jun NH_2-kinase/c-Jun pathway (59). c-Jun NH_2-kinase is activated by ROS and is part of the antioxidant response element–mediated transcriptional response that is a major stimulus for protective antioxidant up-regulation (36). It is possible that ROS- and platinum drug–mediated JNK activation may also induce 8-oxodG–directed BER activity as a cell survival mechanism.

NER and MMR capacities are associated with altered tumor response to cisplatin and oxaliplatin, with lowered NER and functional MMR correlating to increased drug activity (22, 30, 31). We show that BER-mediated repair of the 8-oxodG lesion is an additional determinant of treatment response. It is anticipated that human tumors expressing high levels of OGG1 such as the colorectal adenomas and carcinomas described by Sæbø et al. (60) would exhibit increased resistance to cisplatin, and perhaps oxaliplatin to a lesser extent. The effect of transgenic OGG1 expression in these tissues could be variable. BER capacity may also influence cancer susceptibility in a paradoxical manner, with lowered BER promoting tumor incidence and progression through unchecked oxidative DNA damage. Epidemiologic investigations of genetic BER polymorphisms and cancer risk by Hung et al. (20) indicate that the functionally inhibitory OGG1 Ser326Cys polymorphism correlates with a small but significant increase in cancer incidence, particularly for lung adenocarcinoma (19). Our observations suggest that specific OGG1-directed repair of 8-oxodG may also modulate tumor response to oxidative stress and DNA damage-inducing therapies. The glycosylase/AP lyase reaction at the 8-oxodG lesion creates a single strand break that must be subsequently repaired by other downstream BER enzymes to complete repair (44, 51). Therefore, a high level of Fpg or OGG1 activity may promote cytotoxic DNA damage via accumulation of single strand breaks. Zhang et al. (17) have reported enhanced cisplatin cytotoxicity upon the specific overexpression of OGG1 in mitochondria; an observation that conflicts with our findings. In that study, an alternate isoform of OGG1 was ectopically expressed (β-OGG1; transcript variant 2a) that may have varying 8-oxodG glycosylase activity compared with α-OGG1 (38), and this β-OGG1 was targeted to the mitochondrial matrix. Certainly cell type and environment, the subcellular localization of 8-oxodG glyosylase/AP lyase activity, and the level of this activity relative to activity of other BER enzymes all can act as determinants of cellular response.

This is the first study to show 8-oxodG level induction by oxaliplatin treatment, and to implicate 8-oxodG as a pathogenic macromolecular lesion in the mechanism of platinum compound-induced cytotoxicity. Unlike the proven mutagenic role of 8-oxodG in the initiation of cancer, the underlying mechanism of cytotoxicity involves nonmutagenic effects of 8-oxodG, as two rounds of cell mitosis are required for G:C to A:T transversion mutation and toxicity occurred within hours after treatment. Such 8-oxodG–mediated effects could include induction of stress responses

and alterations in gene expression. This would be consistent with the known effects of 8-oxodG in stalling RNA polymerase and altering the binding of nuclear transcription factors to DNA (61, 62). Additionally, BER capacity as determined by 8-oxoguanine glycosylase/AP lyase activity is identified as a protective factor against this toxicity. Up-regulation of BER reduced cytotoxicity from ROS, a ROS-initiating quinone and platinum compounds, and the resistance to cisplatin was significantly higher than resistance to oxaliplatin. As well, only oxaliplatin treatment produced a prolonged cytostatic effect lasting several days after treatment. This differential response is independent of the comparable levels of ROS and 8-oxodG induction observed from both cisplatin and oxaliplatin exposures. Such distinct oxaliplatin effects seem to diminish the contribution of 8-oxodG accumulation to its specific mechanisms of cytotoxicity. These findings indicate that the potency of oxaliplatin therapy against cisplatin-resistant cancers is distinct from the induction of 8-oxodG. Therefore, the use of anticancer drugs less reliant upon oxidative DNA damage for the induction of target cell death may represent a therapeutic strategy for reducing tumor resistance to therapy.

Disclosure of Potential Conflicts of Interest

No potential conflicts of interest were disclosed.

References

1. Gros L, Saparbaev MK, Laval J. Enzymology of the repair of free radicals-induced DNA damage. Oncogene 2002;21:8905–25.

2. Lindahl T. Instability and decay of the primary structure of DNA. Nature 1993;362:709–15.

3. Klaunig JE, Kamendulis LM. The role of oxidative stress in carcinogenesis. Annu Rev Pharmacol Toxicol 2004;44:239–67.

4. Boiteux S, Radicella JP. The human ogg1 gene: structure, functions, and its implication in the process of carcinogenesis. Arch Biochem Biophys 2000;377:1–8.

5. Bohr VA, Stevnsner T, de Souza-Pinto NC. Mitochondrial DNA repair of oxidative damage in mammalian cells. Gene 2002;286:127–34.

6. Fortini P, Parlanti E, Sidorkina OM, Laval J, Dogliotti E. The type of DNA glycosylase determines the base excision repair pathway in mammalian cells. J Biol Chem 1999;274:15230–6.

7. Nishimura S. Involvement of mammalian ogg1 (mmh) in excision of the 8-hydroxyguanosine residue in DNA. Free Radic Biol Med 2002;32:813–21.

8. Rosenquist TA, Zharkov DO, Grollman AP. Cloning and characterization of a mammalian 8-oxoguanine glycosylase. Proc Natl Acad Sci U S A 1997;94:7429–34.

9. Roldán-Arjona T, Wei Y-F, Carter KC, et al. Molecular cloning and functional expression of a human cDNA encoding the antitumor enzyme 8-hydroxyguanine-DNA glycosylase. Proc Natl Acad Sci U S A 1997;94:8016–20.

10. Chetsanga CJ, Lindahl T. Release of 7-methylguanine residues whose imidazole rings have been opened from damaged DNA by a DNA glycosylase from Escherichia coli. Nucleic Acids Res 1979;6:3673–84.

11. Boiteux S, O'Connor TR, Lederer F, Gouyette A, Laval J. Homogeneous Escherichia coli FPG protein. A DNA glycosylase which excises imidazole ring-opened purines and nicks DNA at apurinic/apyrimidinic sites. J Biol Chem 1990;265:3916–22.

12. Hollenbach S, Dhenaut A, Eckert I, Radicella JP, Epe B. Overexpression of ogg1 in mammalian cells: effects on induced and spontaneous oxidative DNA damage and mutagenesis. Carcinogenesis 1999;20:1863–8.

13. He YH, Xu Y, Kobune M, Wu M, Kelley MR, Martin WJ. Escherichia coli fpg and human ogg1 reduce DNA damage and cytotoxicity by bcnu in human lung cells. Am J Physiol Lung Cell Mol Physiol 2002;282:L50–5.

14. Laposa RR, Henderson JT, Wells PG. Tetracycline-dependent regulation of formamidopyrimidine DNA glycosylase in transgenic mice conditionally reduces oxidative DNA damage *in vivo*. FASEB J 2003;17:1343–5.

15. Osterod M, Hollenbach S, Hengstler JG, Barnes DE, Lindahl T, Epe B. Age-related and tissue-specific accumulation of oxidative DNA base damage in 7,8-dihydro-8-oxoguanine-DNA glycosylase (ogg1) deficient mice. Carcinogenesis 2001;22:1459–63.

16. Arai T, Kelly VP, Minowa O, Noda T, Nishimura S. High accumulation of oxidative DNA damage, 8-hydroxyguanine, in mmh/ogg1 deficient mice by chronic oxidative stress. Carcinogenesis 2002;23:2005–10.

17. Zhang H, Mizumachi T, Carcel-Trullols J, et al. Targeting human 8-oxoguanine DNA glycosylase (hOGG1) to mitochondria enhances cisplatin cytotoxicity in hepatoma cells. Carcinogenesis 2007;28:1629–37.

18. Audebert M, Chevillard S, Levalois C, et al. Alterations of the DNA repair gene ogg1 in human clear cell carcinomas of the kidney. Cancer Res 2000;60:4740–4.

19. Goode EL, Ulrich CM, Potter JD. Polymorphisms of DNA repair genes and associations with cancer risk. Cancer Epidemiol Biomarkers Prev 2002;11:1513–30.

20. Hung RJ, Brennan P, Canzian F, et al. Large-scale investigation of base excision repair polymorphisms and lung cancer risk in a multicenter study. J Natl Cancer Inst 2005;97:567–76.

21. Wang D, Lippard SJ. Cellular processing of platinum anticancer drugs. Nat Rev Drug Discov 2005;4:307–20.

22. Stojic L, Brun R, Jiricny J. Mismatch repair and DNA damage signaling. DNA Repair (Amst) 2004;3:1091–101.

23. Goodisman J, Hagrman D, Tacka KA, Souid A-K. Analysis of cytotoxicities of platinum compounds. Cancer Chemother Pharmacol 2006;57:257–67.

24. Bratasz A, Weir NM, Parinandi NL, et al. Reversal to cisplatin sensitivity in recurrent human ovarian cancer cells by NCX-4016, a nitro derivative of aspirin. Proc Natl Acad Sci U S A 2006;103:3914–9.

25. Baek SM, Kwon CH, Kim JH, Woo JS, Jung JS, Kim YK. Differential roles of hydrogen peroxide and hydroxyl radical in cisplatin-induced cell death in renal proximal tubular epithelial cells. J Lab Clin Med 2003;142:178–86.

26. Wu YJ, Muldoon LL, Neuwelt EA. The chemoprotective agent *N*-acetylcysteine blocks cisplatin-induced apoptosis through caspase signaling pathway. J Pharmacol Exp Ther 2005;312:424–31.

27. Satoh M, Kashihara N, Fujimoto S, et al. A novel free radical scavenger, edarabone, protects against cisplatin-induced acute renal damage *in vitro* and *in vivo*. J Pharmacol Exp Ther 2003;305:1183–90.

28. Atessahin A, Yilmaz S, Karahan I, Ceribasi AO, Karaoglu A. Effects of lycopene against cisplatin-induced nephrotoxicity and oxidative stress in rats. Toxicology 2005;212:116–23.

29. Rixe O, Ortuzar W, Alvarez M, et al. Oxaliplatin, tetraplatin, cisplatin, and carboplatin: spectrum of activity in drug-resistant cell lines and the cell lines of the National Cancer Institute's Anticancer Drug Screen panel. Biochem Pharmacol 1996;52:1855–65.

30. Raymond E, Faivre S, Chaney S, Woynarowski J, Cvitkovic E. Cellular and molecular pharmacology of oxaliplatin. Mol Cancer Ther 2002;1:227–35.

31. Viguier J, Boige V, Miquel C, et al. *ERCC1* codon 118 polymorphism is a predictive factor for the tumor response to oxaliplatin/5-fluorouracil combination chemotherapy in patients with advanced colorectal cancer. Clin Cancer Res 2005;11:6212–7.

32. Lin PC, Lee MY, Wang WS, et al. *N*-acetlycysteine has neuroprotective effects against oxaliplatin-based adjuvant chemotherapy in colon cancer patients: preliminary data. Support Care Cancer 2006;14:484–7.

33. Watanabe N, Dickinson DA, Liu R-M, Forman HJ. Quinones and glutathione metabolism. Methods Enzymol 2004;378:319–40.

34. Niwa H, Yamamura K-i, Miyajaki J-i. Efficient selection for high-expression transfectants with a novel eukaryotic vector. Gene 1991;108:193–200.

35. Dobson AW, Xu Y, Kelley MR, LeDoux SP, Wilson GL. Enhanced mitochondrial DNA repair and cellular survival after oxidative stress by targeting the human 8-oxoguanine glycosylase repair enzyme to mitochondria. J Biol Chem 2000;275:37518–23.

36. Preston TJ, Woodgett JR, Singh G. JNK1 activity lowers the cellular production of H_2O_2 and modulates the growth arrest response to scavenging of H_2O_2 by catalase. Exp Cell Res 2003;285:146–58.

37. Ravanat JL, Douki T, Duez P, et al. Cellular background level of 8-oxo-7,8-dihydro-2′-deoxyguanosine: an isotope based method to evaluate artefactual oxidation of DNA during its extraction and subsequent work-up. Carcinogenesis 2002;23:1911–8.

38. Hashiguchi K, Stuart JA, deSuoza-Pinto NC, Bohr VA. The C-terminal α0 helix of human Ogg1 is essential for 8-oxoguanine DNA glycosylase activity: the mitochondrial β-Ogg1 lacks this domain and does not have glycosylase activity. Nucleic Acids Res 2004;32:5596–608.

39. Kharbanda S, Saxena S, Kiyotsugu Y, et al. Translocation of SAPK/JNK to mitochondria and interaction with Bcl-x_L in response to DNA damage. J Biol Chem 2000;275:322–7.

40. Aoki H, Kang PM, Hampe J, et al. Direct activation of mitochondrial apoptosis machinery by c-Jun N-terminal Kinase in adult cardiac myocytes. J Biol Chem 2002;277:10244–50.

41. Eminel S, Klettner A, Roemer L, Herdegen T, Waetzig V. JNK2 translocates to the mitochondria and mediates cytochrome c release in PC12 cells in response to 6-hydroxydopamine. J Biol Chem 2004;279:55385–92.

42. Xiao W, Samson L. *In vivo* evidence for endogenous DNA alkylation damage as a source of spontaneous mutation in eukaryotic cells. Proc Natl Acad Sci U S A 1993;90:2117–21.

43. Yang N, Galick H, Wallace SS. Attempted base excision repair of ionizing radiation damage in human lymphoblastoid cells produces lethal and mutagenic double strand breaks. DNA Repair (Amst) 2004;3:1323–34.

44. Yang N, Chaudhry MA, Wallace SS. Base excision repair by NTH1 and hOGG1: a two edged sword in the processing of DNA damage in γ-irradiated human cells. DNA Repair (Amst) 2006;5:43–51.

45. Yamane A, Shinmura K, Sunaga N, et al. Suppresive activities of OGG1 and MYH proteins against G:C to T:A mutations caused by 8-hydroxyguanine but not by benzo[a]pyrene diol epoxide in human cells *in vivo*. Carcinogenesis 2003;24:1031–7.

46. Blaisdell JO, Wallace SS. Abortive base excision repair of radiation-induced clustered DNA lesions in Escherichia coli. Proc Natl Acad Sci U S A 2001;98:7426–30.

47. Holt SM, Georgakalis AG. Detection of complex DNA damage in γ-irradiated acute lymphoblastic leukemia pre-B NALM-6 cells. Radiat Res 2007;168:527–34.

48. Georgakalis AG, Bennett PV, Wilson DM, III, Sutherland BM. Processing of bistranded abasic DNA clusters in γ-irradiated human hematopoietic cells. Nucleic Acids Res 2004;32:5609–20.

49. Hill JW, Hu JJ, Evans MK. OGG1 is degraded by calpain following oxidative stress and cisplatin exposure. DNA Repair (Amst) 2008;7:648–54.

50. Laurent A, Nicco C, Chéreau C, et al. Controlling tumor growth by modulating endogenous production of reactive oxygen species. Cancer Res 2005;65:948–56.

51. Hill JW, Hazra TK, Izumi T, Mitra S. Stimulation of human 8-oxoguanine-DNA glycosylase by AP-endonuclease: potential coordination of the initial steps in base excision repair. Nucleic Acids Res 2001;29:430–8.

52. Pabla N, Huang S, Mi QS, Daniel R, Dong Z. ATR-Chk2 signaling in p53 activation and DNA damage response during cisplatin-induced apoptosis. J Biol Chem 2008;283:6572–83.

53. Miglietta L, Franzone P, Centurioni MG, et al. A phase II trial with cisplatin-paclitaxel cytotoxic treatment and concurrent external and endocavitary radiation therapy in locally advanced or recurrent cervical cancer. Oncology 2006;70:19–24.

54. Carlomagno C, Orditura M, Pepe S, et al. Capecitabine plus weekly oxaliplatin in gastrointestinal tumors: a phase I study. Am J Clin Oncol 2006;29:85–9.

55. Paul S, Gros L, Laval J, Sutherland BM. Expression of the E. coli Fpg protein in CHO cells lowers endogenous oxypurine clustered DNA damage levels and decreases accumulation of endogenous Hprt mutations. Environ Mol Mutagen 2006;47:311–9.

56. Engel RH, Evens AM. Oxidative stress and apoptosis: a new treatment paradigm in cancer. Front Biosci 2006;11:300–12.

57. Wells PG, McCallum GP, Chen CS, et al. Oxidative stress in developmental origins of disease: teratogenesis, neurodevelopmental deficits and cancer. Toxicol Sci 2009;108:4–18.

58. Jeng W, Ramkissoon A, Parman T, Wells PG. Prostaglandin H synthase-catalyzed bioactivation of amphetamines to free radical intermediates that cause CNS regional DNA oxidation and nerve terminal degeneration. FASEB J 2006;20:638–50.

59. Potapova O, Haghighi A, Bost F, et al. The Jun kinase/stress-activated protein kinase pathway functions to regulate DNA repair and inhibition of the pathway sensitizes tumor cells to cisplatin. J Biol Chem 1997;272:14041–4.

60. Sæbø M, Skjelbred CF, Nexø BA, et al. Increased mRNA expression levels of *ERCC1, OGG1* and *RAI* in colorectal adenomas and carcinomas. BMC Cancer 2006;6:208.

61. Viswanathan A, Doetsch PW. Effects of nonbulky DNA base damages on Escherichia coli RNA polymerase-mediated elongation and promoter clearance. J Biol Chem 1998;273:21276–81.

62. Hailer-Morrison MK, Kotler JM, Martin BD, Sugden KD. Oxidized guanine lesions as modulators of gene transcription. Altered p50 binding affinity and repair shielding by 7,8-dihydro-8-oxo-2′-deoxyguanosine lesions in the NF-κB promoter element. Biochemistry 2003;42:9761–70.